

Appendix to:

C.A.J. Appelo, Principles, caveats and improvements in databases for calculating hydrogeochemical reactions in saline waters from 0 - 200 °C and 1 - 1000 atm.

This appendix has figures showing experimental solubilities and PHREEQC calculations, using the Pitzer interaction coefficients given in Table 1, and the temperature dependent log  $K$ 's in Table 2 of the paper. The PHREEQC input files are in the directory:

c:\phreeqc\high\_P\_T\appendix\_AG15

The main directory contains pitzer.dat and input files that calculate the figures presented by Pabalan and Pitzer, 1987. Input files for other minerals and CO<sub>2</sub> gas are in sub-directories.

It is easiest to run the files with Notepad++ adapted for PHREEQC. Download from:

<http://www.hydrochemistry.eu/ph3/phreeqc3.Installer.exe>

and install in your computer. In Notepad++, open a file (Ctrl+O), and press Ctrl+F6 to start the PHREEQC calculations.

Table 3. List of figures with mineral solubilities as a function of  $T$ ,  $P$  and solution composition.

| Mineral solubility in water or aqueous solution   | Temp °C   | Pressure atm  | Figure |
|---|-----------|---------------|--------|
| halite (NaCl)   | 0 - 300   | 1 - $P_{sat}$ | A1     |
| sylvite (KCl)   | 10 - 300  | 1 - $P_{sat}$ | A2     |
| bischofite (MgCl <sub>2</sub> :6H <sub>2</sub> O), MgCl <sub>2</sub> :2H <sub>2</sub> O, MgCl <sub>2</sub> :4H <sub>2</sub> O   | 0 - 200   | 1 - $P_{sat}$ | A3     |
| mirabilite (Na <sub>2</sub> SO <sub>4</sub> :10H <sub>2</sub> O), thenardite (Na <sub>2</sub> SO <sub>4</sub> )   | 0 - 220   | 1 - $P_{sat}$ | A4     |
| arcanite (K <sub>2</sub> SO <sub>4</sub> )  | 0 - 210   | 1 - $P_{sat}$ | A5     |
| epsomite (MgSO <sub>4</sub> :7H <sub>2</sub> O), hexahydrate (MgSO <sub>4</sub> :6H <sub>2</sub> O), kieserite (MgSO <sub>4</sub> :H <sub>2</sub> O)  | 0 - 200   | 1 - $P_{sat}$ | A6     |
| halite (NaCl), sylvite (KCl) in Na/K-Cl solutions   | 0 - 200   | 1 - $P_{sat}$ | A7     |
| carnallite (KMgCl <sub>3</sub> :H <sub>2</sub> O) in K/Mg-Cl solutions  | 0 - 75    | 1             | A8     |
| gypsum (CaSO <sub>4</sub> :2H <sub>2</sub> O)   | 0 - 95    | 1             | A9     |
| gypsum (CaSO <sub>4</sub> :2H <sub>2</sub> O) in NaCl solutions   | 0.5 - 95  | 1             | A10    |
| gypsum (CaSO <sub>4</sub> :2H <sub>2</sub> O), mirabilite (Na <sub>2</sub> SO <sub>4</sub> :10H <sub>2</sub> O), glauberite (Na <sub>2</sub> Ca(SO <sub>4</sub> ) <sub>2</sub> ) and thenardite (Na <sub>2</sub> SO <sub>4</sub> ) in Na <sub>2</sub> SO <sub>4</sub> solutions | 25 - 100  | 1             | A11    |
| gypsum (CaSO <sub>4</sub> :2H <sub>2</sub> O) and anhydrite (CaSO <sub>4</sub> )  | 30 - 160  | 1 - 1000      | A12    |
| anhydrite (CaSO <sub>4</sub> ) in NaCl solutions  | 100 - 200 | 1 - $P_{sat}$ | A13    |
| anhydrite (CaSO <sub>4</sub> ) in NaCl solutions  | 100 - 200 | 1 - 987       | A14    |
| anhydrite (CaSO <sub>4</sub> ) and glauberite (Na <sub>2</sub> Ca(SO <sub>4</sub> ) <sub>2</sub> ) in Na <sub>2</sub> SO <sub>4</sub> solutions   | 100 - 200 | 1 - $P_{sat}$ | A15    |
| anhydrite (CaSO <sub>4</sub> ), Goergeyite (K <sub>2</sub> Ca <sub>5</sub> (SO <sub>4</sub> ) <sub>6</sub> H <sub>2</sub> O) and syngenite (K <sub>2</sub> Ca(SO <sub>4</sub> ) <sub>2</sub> :H <sub>2</sub> O) in K <sub>2</sub> SO <sub>4</sub> solutions                     | 100 - 200 | 1 - $P_{sat}$ | A16    |
| amorphous silica (SiO <sub>2</sub> (a)) in NaCl solutions   | 25 - 300  | 1 - $P_{sat}$ | A17    |
| amorphous silica (SiO <sub>2</sub> (a)) in Na <sub>2</sub> SO <sub>4</sub> solutions  | 25 - 300  | 1 - $P_{sat}$ | A18    |
| amorphous silica (SiO <sub>2</sub> (a)) in MgCl <sub>2</sub> solutions  | 25 - 300  | 1 - $P_{sat}$ | A19    |
| amorphous silica (SiO <sub>2</sub> (a)) in MgSO <sub>4</sub> solutions  | 25 - 250  | 1 - $P_{sat}$ | A20    |
| amorphous silica (SiO <sub>2</sub> (a)) in Li-Cl/NO <sub>3</sub> solutions  | 25        | 1             | A21    |

|  |           |                            |     |
|--|-----------|----------------------------|-----|
| amorphous silica ( $\text{SiO}_2(\text{a})$ ) in K-Cl/ $\text{NO}_3$ solutions | 25        | 1                          | A22 |
| amorphous silica ( $\text{SiO}_2(\text{a})$ ) in $\text{CaCl}_2$ solutions     | 25        | 1                          | A23 |
| barite ( $\text{BaSO}_4$ ) in NaCl solutions                                   | 1 - 250   | $1 - P_{\text{sat}}$       | A24 |
| barite ( $\text{BaSO}_4$ ) in NaCl solutions                                   | 150 - 250 | 493                        | A25 |
| calcite ( $\text{CaCO}_3$ ) in NaCl solutions                                  | 10 - 60   | 1                          | A26 |
| calcite ( $\text{CaCO}_3$ ) in 3 M NaCl, variable $\text{CO}_2$                | 200       | 580                        | A27 |
| calcite ( $\text{CaCO}_3$ ) in NaCl solutions                                  | 120 - 260 | 12                         | A28 |
| calcite ( $\text{CaCO}_3$ ) at 1 bar $\text{CO}_2$ pressure                    | 0 - 300   | $1 - (P_{\text{sat}} + 1)$ | A29 |
| calcite ( $\text{CaCO}_3$ ) in NaCl solutions at 1 bar $\text{CO}_2$ pressure  | 0 - 250   | 1 - 1450                   | A30 |
| $\text{CO}_2$ gas  | 25 - 100  | 1 - 710                    | A31 |
| $\text{CO}_2$ gas in 1 and 6 M NaCl solution                                   | 25 - 300  | 35 - 200                   | A32 |
| $\text{CO}_2$ gas in 4 M NaCl solution   | 80 - 180  | 9 - 95                     | A33 |
| $\text{CO}_2$ gas in $\text{Na}_2\text{SO}_4$ solutions                        | 140       | 12 - 96                    | A34 |
| $\text{CO}_2$ gas in 2.3 M $\text{CaCl}_2$ solution                            | 75 - 120  | 22 - 655                   | A35 |
| $\text{CO}_2$ fugacity coefficients  | 0 - 300   | 99 - 987                   | A36 |

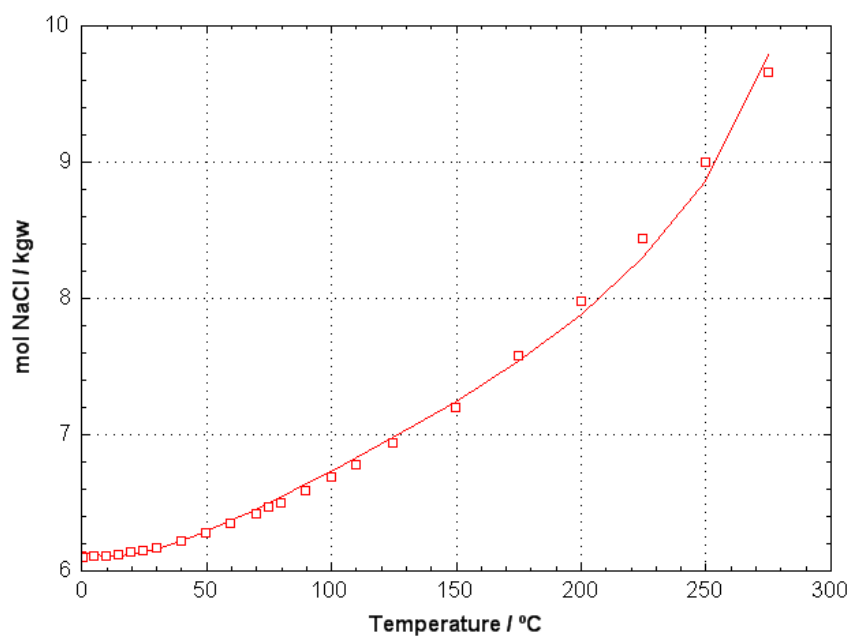


Figure A1. Halite (NaCl) solubility as a function of temperature. Data points from Pabalan and Pitzer, 1987; Clarke and Glew, 1985. File Halite.phr

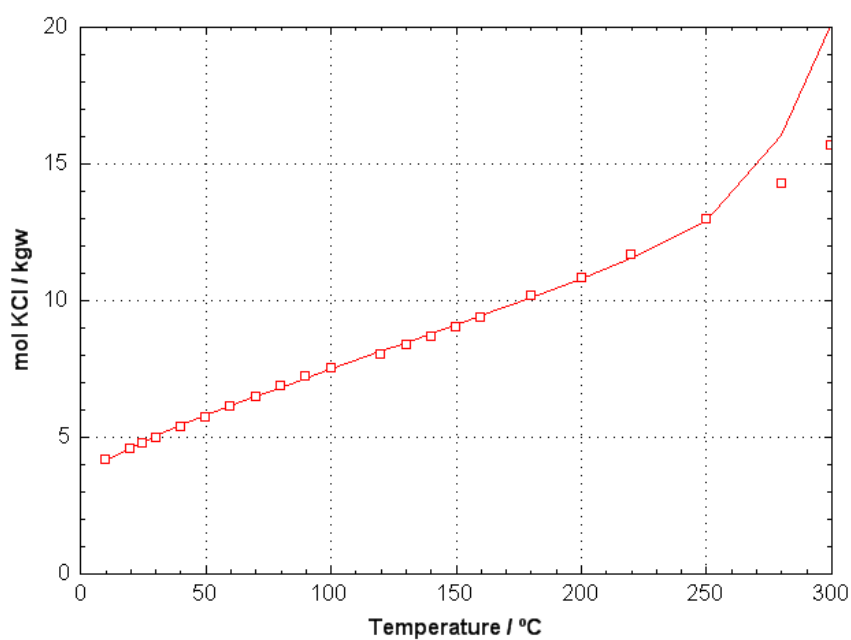


Figure A2. Sylvite (KCl) solubility as a function of temperature. Data points from Pabalan and Pitzer, 1987. File Sylvite.phr

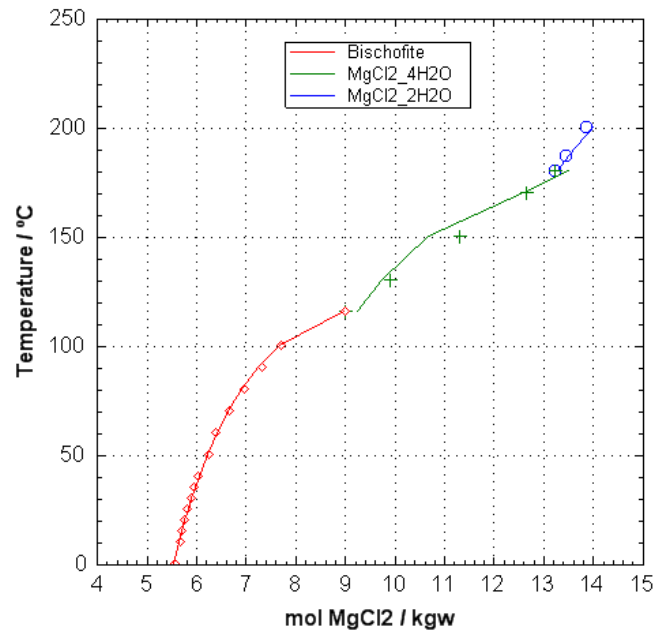


Figure A3. Solubility of  $\text{MgCl}_2$ -hydrates. Data points from Pabalan and Pitzer, 1987. File  $\text{MgCl}_2.\text{phr}$

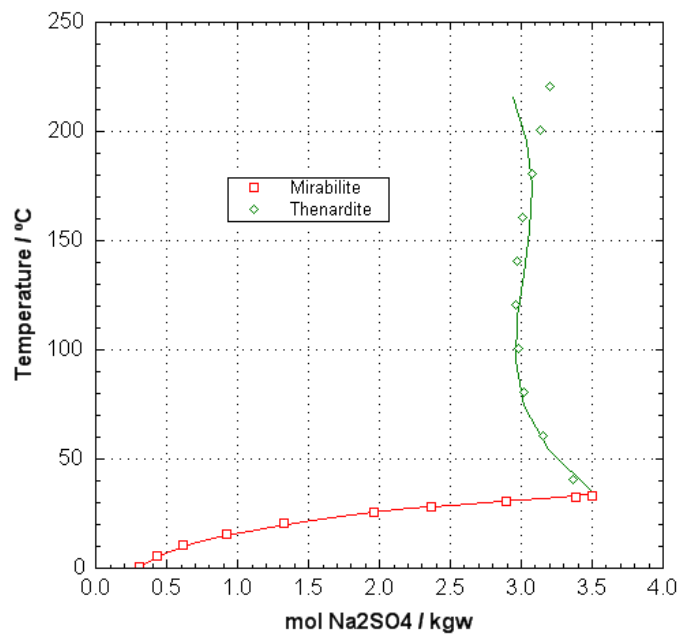


Figure A4. Solubility of  $\text{Na}_2\text{SO}_4$ -(an)hydrate. Data points from Pabalan and Pitzer, 1987. File  $\text{Na}_2\text{SO}_4.\text{phr}$

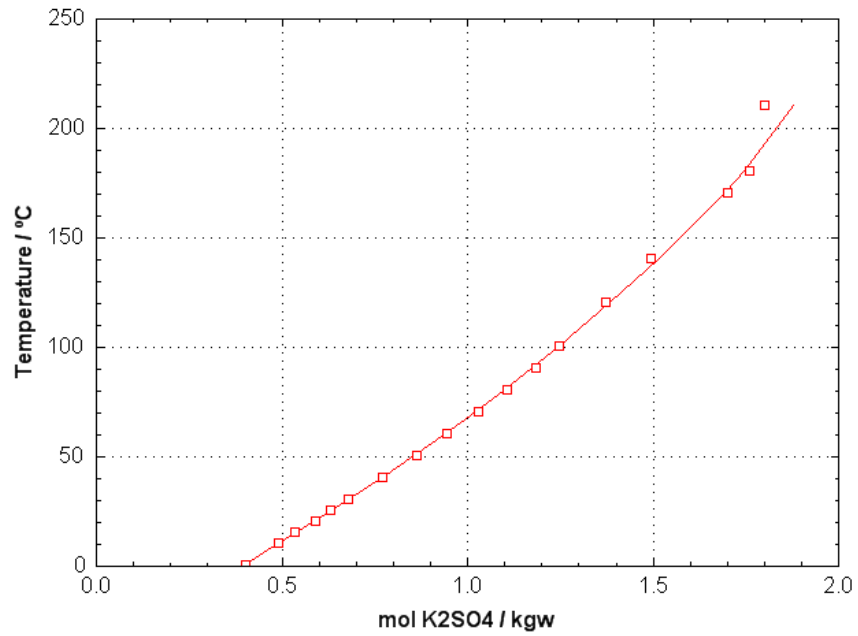


Figure A5. Solubility of arcanite ( $\text{K}_2\text{SO}_4$ ). Data points from Pabalan and Pitzer, 1987. File K2SO4.phr

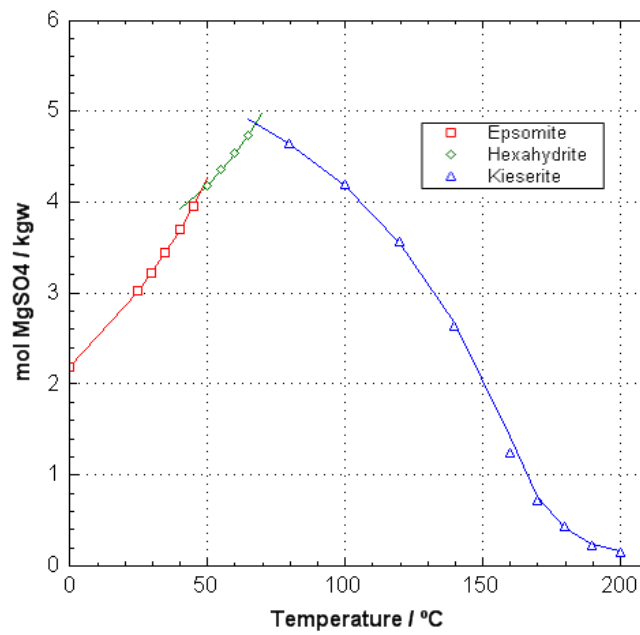


Figure A6. Solubility of  $\text{MgSO}_4$ -hydrates. Data points from Pabalan and Pitzer, 1987. File MgSO4.phr

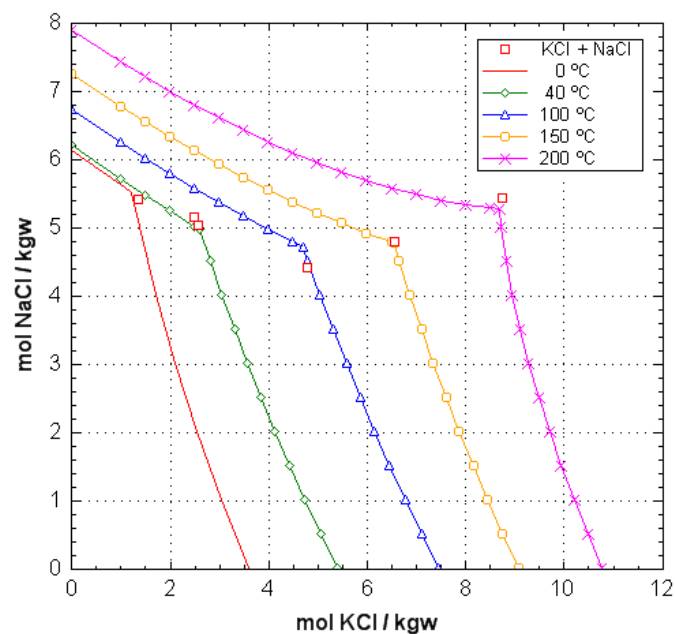


Figure A7. Mutual influence of NaCl and KCl solutions on halite and sylvite solubilities, with triple points KCl + NaCl + H<sub>2</sub>O from Pabalan and Pitzer, 1987. File NaKCl.phr

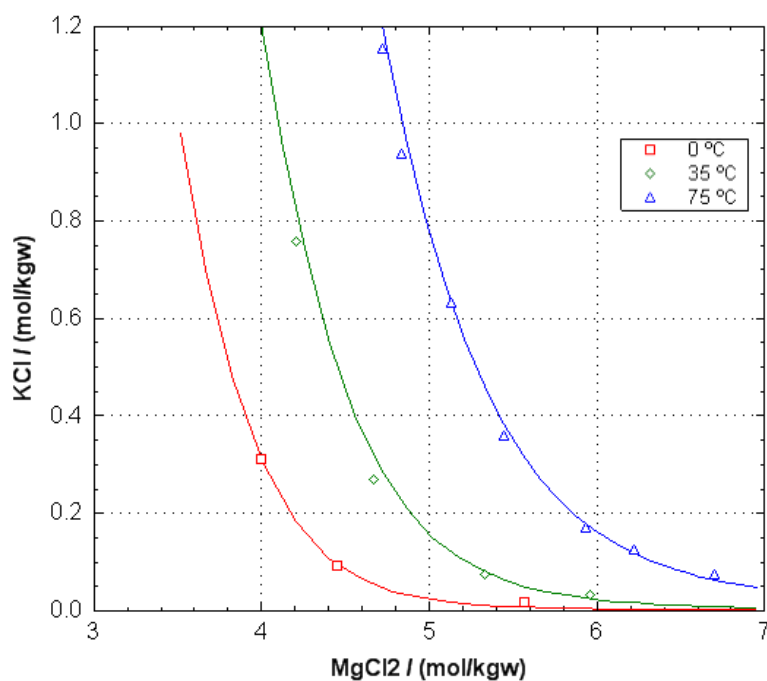


Figure A8. Solubility of carnallite (KMgCl<sub>3</sub>·H<sub>2</sub>O). Data points from Pabalan and Pitzer, 1987. File Carnallite.phr

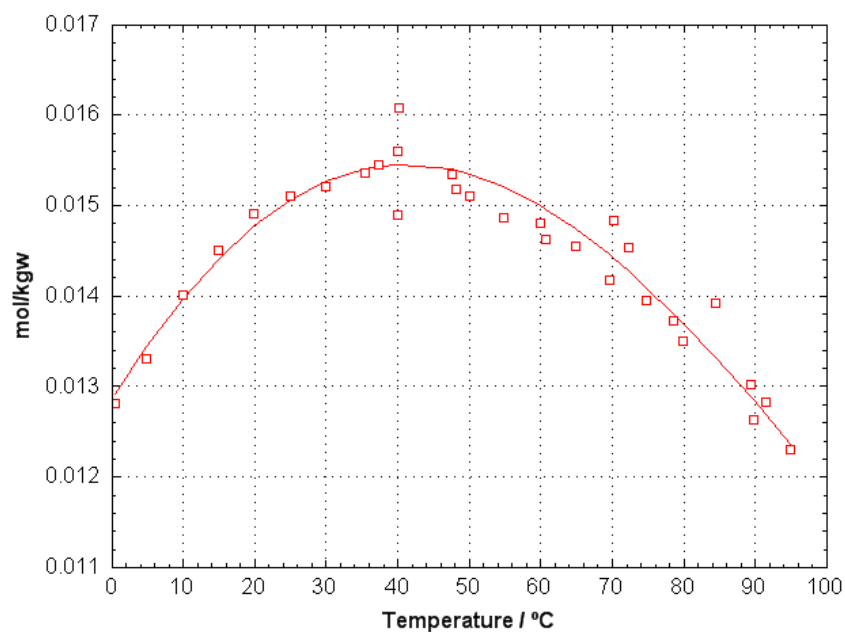


Figure A9. Solubility of gypsum ( $\text{CaSO}_4 \cdot 2\text{H}_2\text{O}$ ). Data points from Marshall and Slusher, 1966; Blount and Dickson, 1969. File gypsum.phr

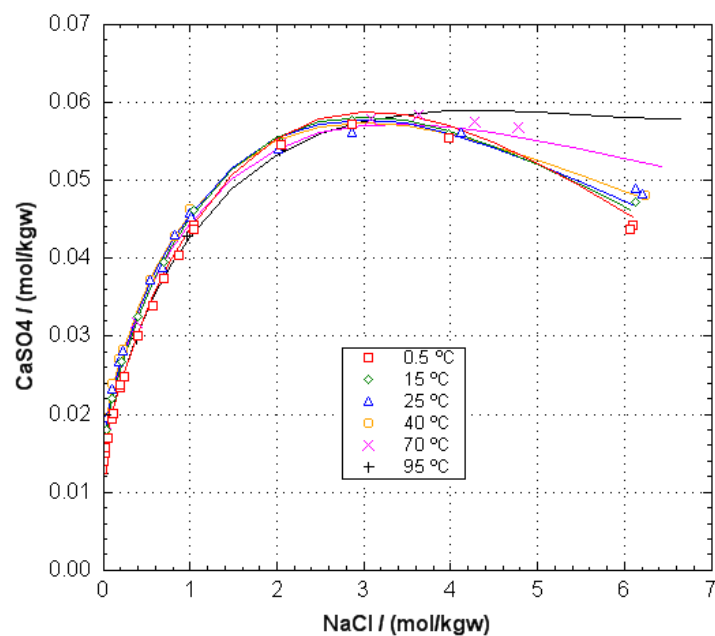


Figure A10. Solubility of gypsum ( $\text{CaSO}_4 \cdot 2\text{H}_2\text{O}$ ) in NaCl solutions. Data points from Marshall and Slusher, 1966. File gyps\_NaCl.phr

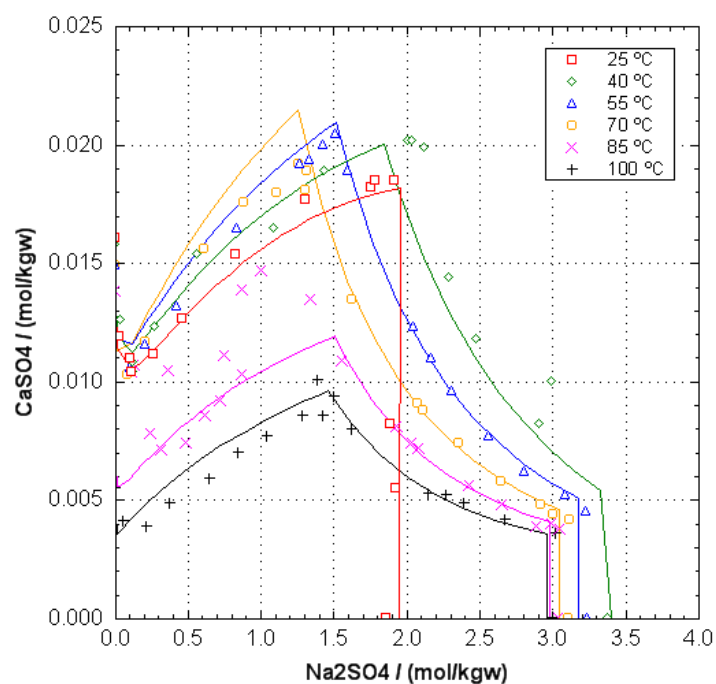


Figure A11. Solubility of gypsum ( $\text{CaSO}_4 \cdot 2\text{H}_2\text{O}$ ) in  $\text{Na}_2\text{SO}_4$  solutions. Data points from Block and Waters, 1968. File gyps\_Na2SO4.phr. The concentration decrease of  $\text{CaSO}_4$  at  $\text{Na}_2\text{SO}_4$  concentrations above 1 M is due to mirabilite precipitation (25°C), or glauberite and thenardite precipitation at higher temperatures. At 85 and 100°C, and possibly at 70°C, gypsum transforms into anhydrite.

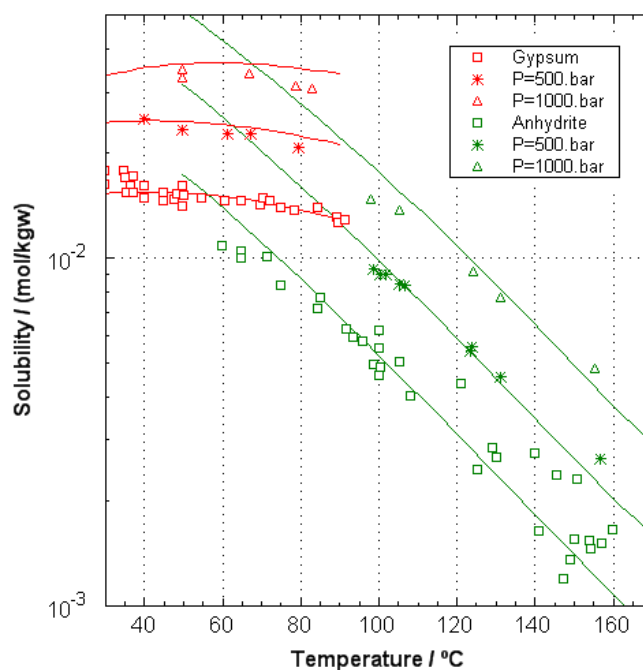


Figure A12. Solubility of gypsum ( $\text{CaSO}_4 \cdot 2\text{H}_2\text{O}$ ) and anhydrite ( $\text{CaSO}_4$ ) as a function of temperature and pressure. Data points from Blount and Dickson, 1973. File gypsum\_P.phr.



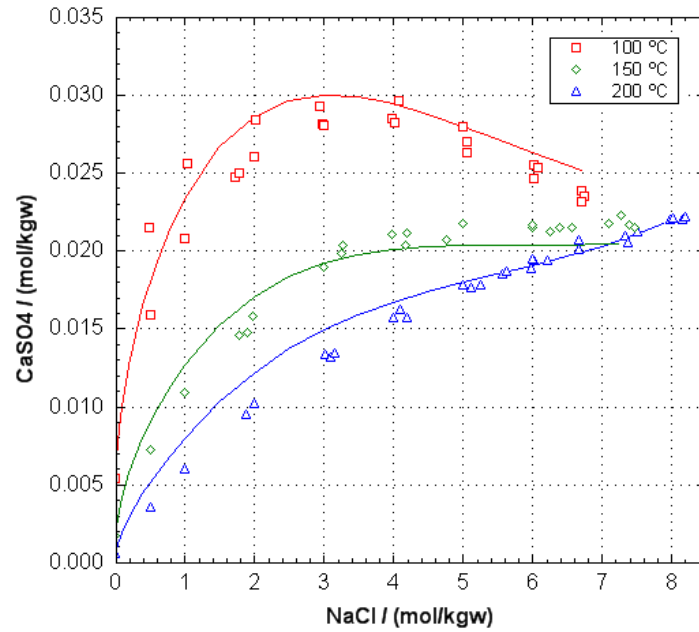


Figure A13. Solubility of anhydrite ( $\text{CaSO}_4$ ) in NaCl solutions. Data points from Block and Waters, 1968; Blount and Dickson, 1969; Freyer and Voigt, 2004. File anhy\_NaCl.phr.

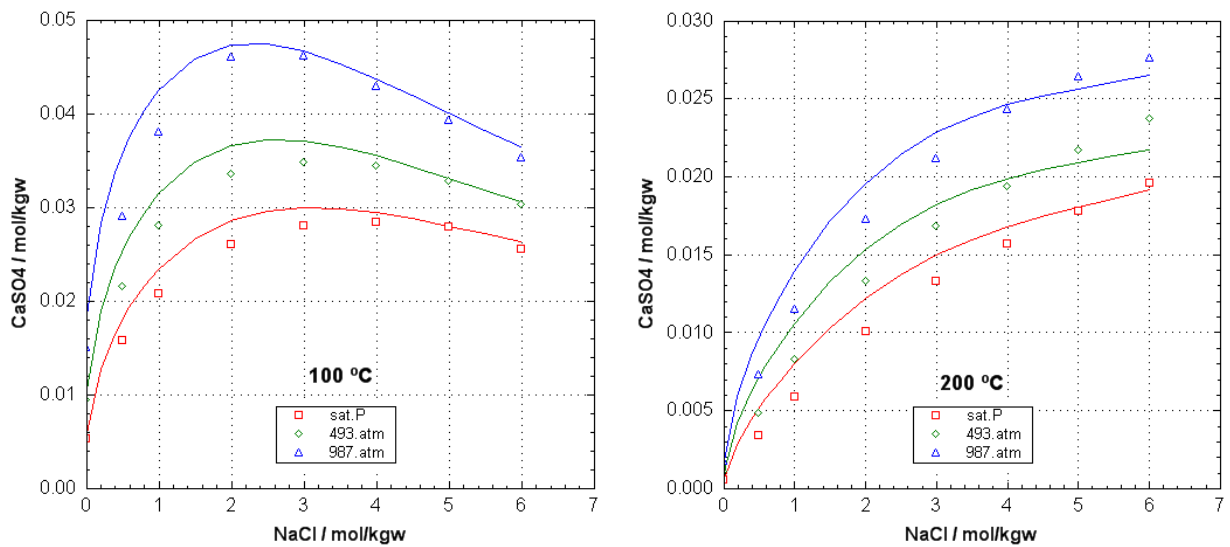


Figure A14. Solubility of anhydrite ( $\text{CaSO}_4$ ) in NaCl solutions as a function of pressure at 100°C and 200°C. Data points from the summary table in Blount and Dickson, 1969. File anhy\_P\_NaCl.phr.

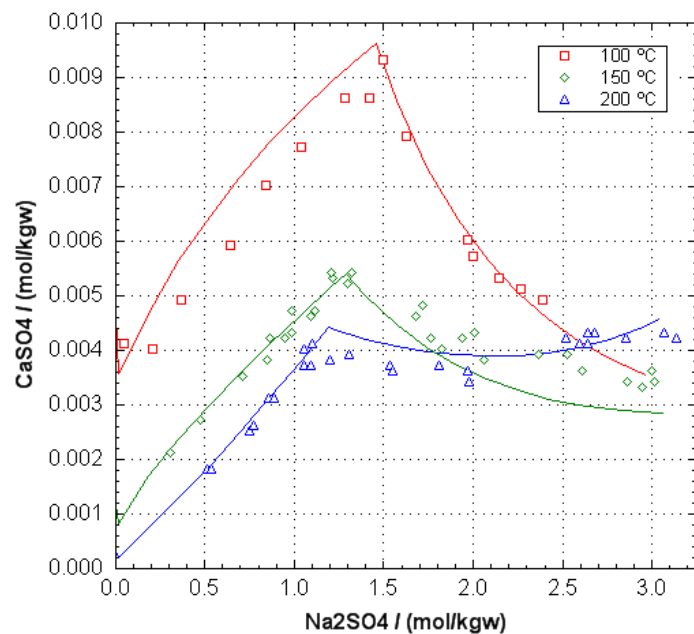


Figure A15. Solubility of anhydrite ( $\text{CaSO}_4$ ) in  $\text{Na}_2\text{SO}_4$  solutions. Data points from Freyer and Voigt, 2004. The decrease of the  $\text{CaSO}_4$  concentration at  $\text{Na}_2\text{SO}_4$  concentrations above 1 M is due to glauberite precipitation. File anhy\_ $\text{Na}_2\text{SO}_4$ .phr.

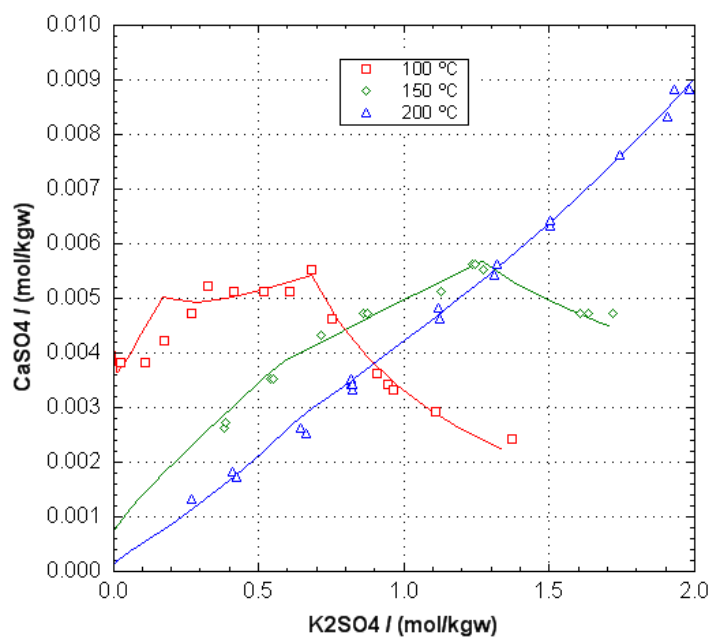


Figure A16. Solubility of anhydrite ( $\text{CaSO}_4$ ) in  $\text{K}_2\text{SO}_4$  solutions. Data points from Freyer and Voigt, 2004. The breaks in the concentration lines result from precipitation of Goergeyite ( $\text{K}_2\text{Ca}_5(\text{SO}_4)_6\text{H}_2\text{O}$ ) and, at 100 and 150°C, Syngenite ( $\text{K}_2\text{Ca}(\text{SO}_4)_2\text{H}_2\text{O}$ ). File anhy\_ $\text{K}_2\text{SO}_4$ .phr.

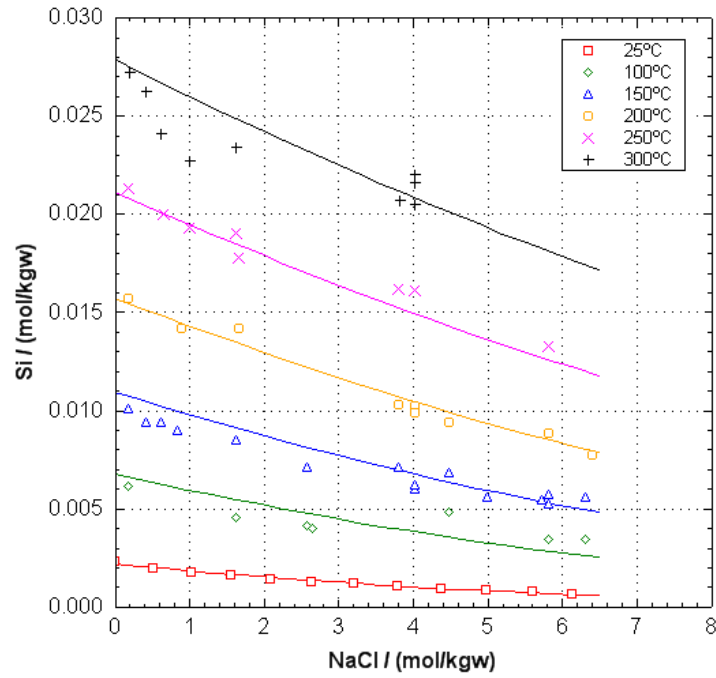


Figure A17. Solubility of amorphous silica ( $\text{SiO}_2(\text{a})$ ) in NaCl solutions. Data points from Marshall and Warakomski, 1980, and Chen and Marshall, 1982. File SiO2\_NaCl.phr.

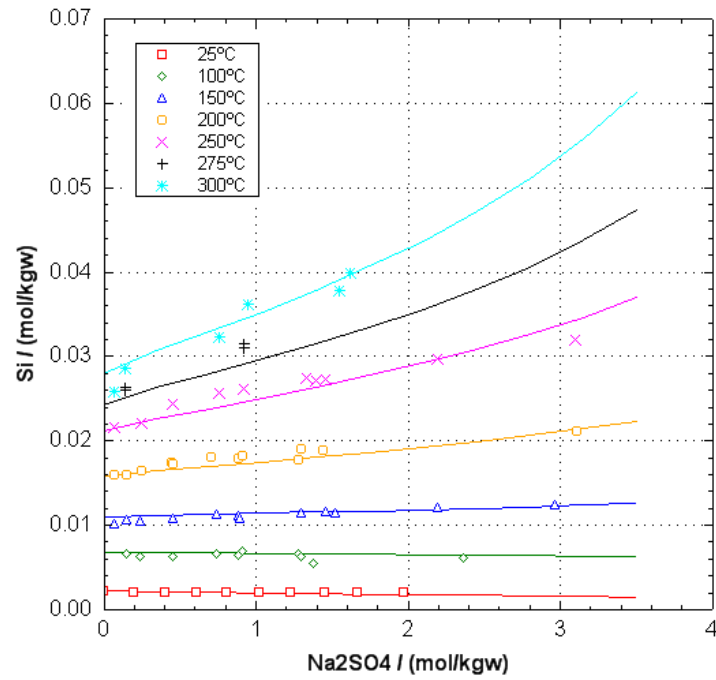


Figure A18. Solubility of amorphous silica ( $\text{SiO}_2(\text{a})$ ) in  $\text{Na}_2\text{SO}_4$  solutions. Data points from Marshall and Warakomski, 1980, and Chen and Marshall, 1982. File SiO2\_Na2SO4.phr.

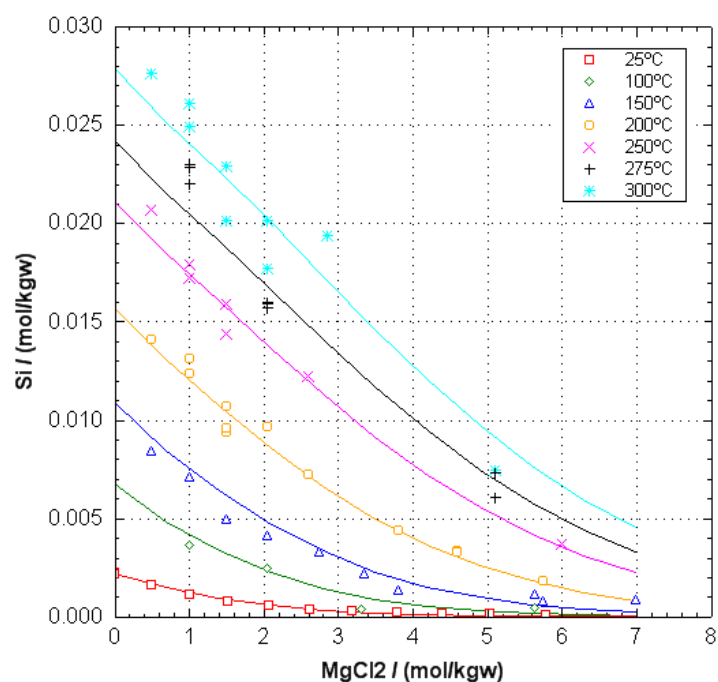


Figure A19. Solubility of amorphous silica ( $\text{SiO}_2(\text{a})$ ) in  $\text{MgCl}_2$  solutions. Data points from Marshall and Warakomski, 1980, and Chen and Marshall, 1982. File  $\text{SiO}_2\_ \text{MgCl}_2.\text{phr}$ .

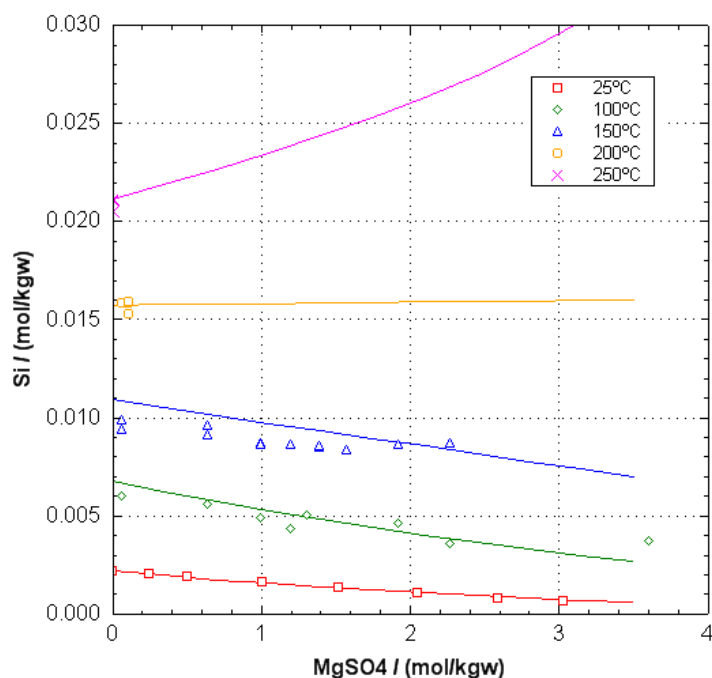


Figure A20. Solubility of amorphous silica ( $\text{SiO}_2(\text{a})$ ) in  $\text{MgSO}_4$  solutions. Data points from Marshall and Warakomski, 1980, and Chen and Marshall, 1982. File  $\text{SiO}_2\_ \text{MgSO}_4.\text{phr}$ .

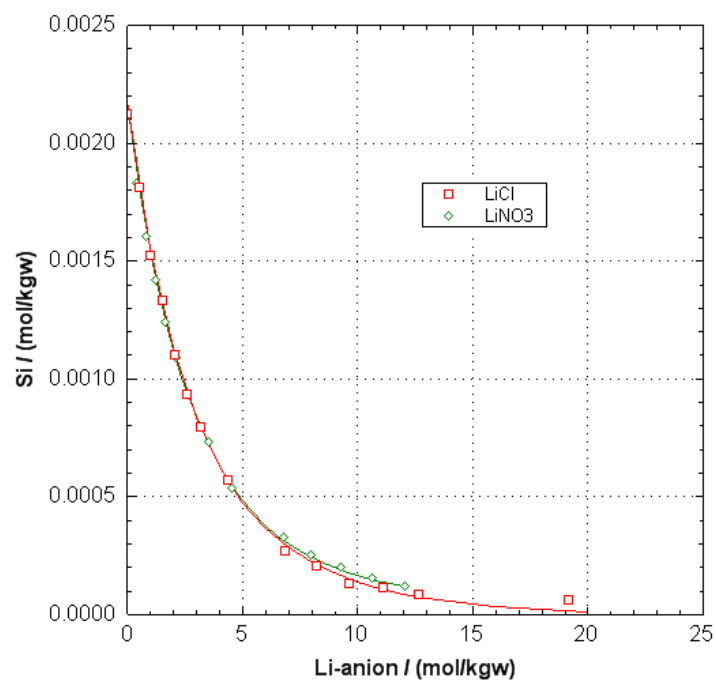


Figure A21. Solubility of amorphous silica ( $\text{SiO}_2(\text{a})$ ) in  $\text{LiCl}$  and  $\text{LiNO}_3$  solutions at  $25^\circ\text{C}$ . Data points from Marshall and Warakowski, 1980. File `SiO2_Li.phr`.

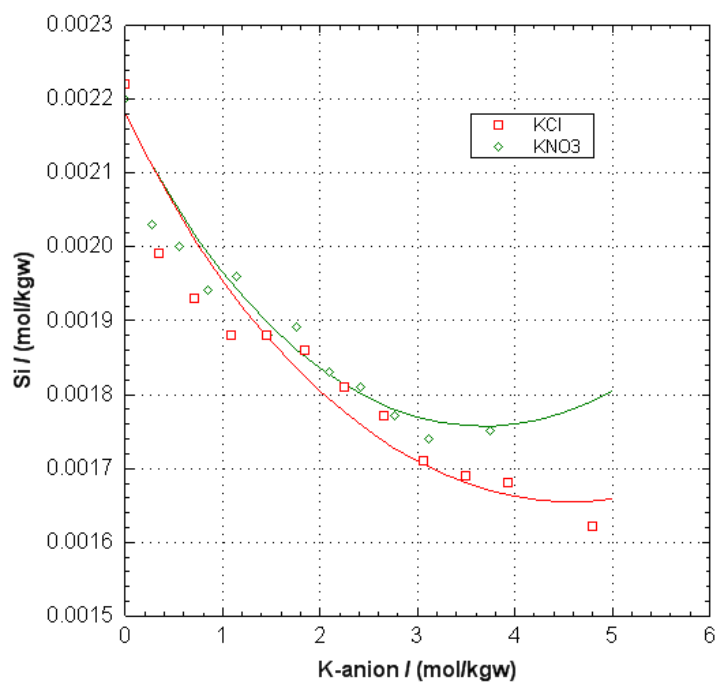


Figure A22. Solubility of amorphous silica ( $\text{SiO}_2(\text{a})$ ) in  $\text{KCl}$  and  $\text{KNO}_3$  solutions at  $25^\circ\text{C}$ . Data points from Marshall and Warakowski, 1980. File `SiO2_K.phr`.

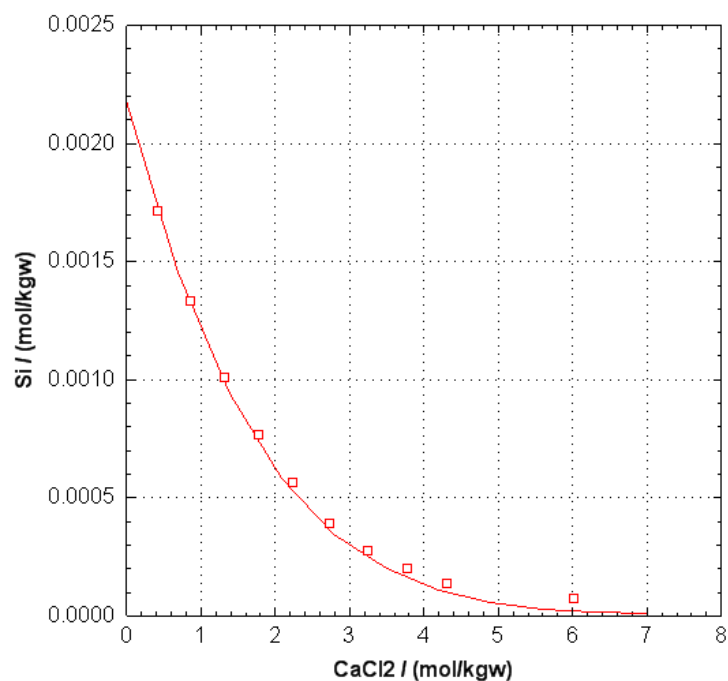


Figure A23. Solubility of amorphous silica ( $\text{SiO}_2(\text{a})$ ) in  $\text{CaCl}_2$  solutions at 25°C. Data points from Marshall and Warakowski, 1980. File `SiO2_CaCl2.phr`.

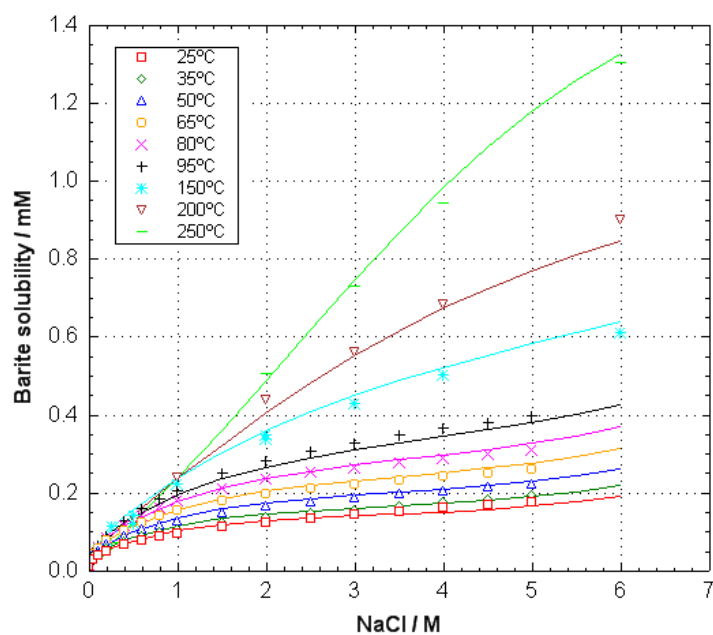


Figure A24. Solubility of barite ( $\text{BaSO}_4$ ) in  $\text{NaCl}$  solutions. Data points  $< 95^\circ\text{C}$  from Templeton, 1960,  $> 100^\circ\text{C}$  from Uchameyshvili et al., 1966, and the summary table in Blount, 1977. File `Barite_NaCl.phr`.

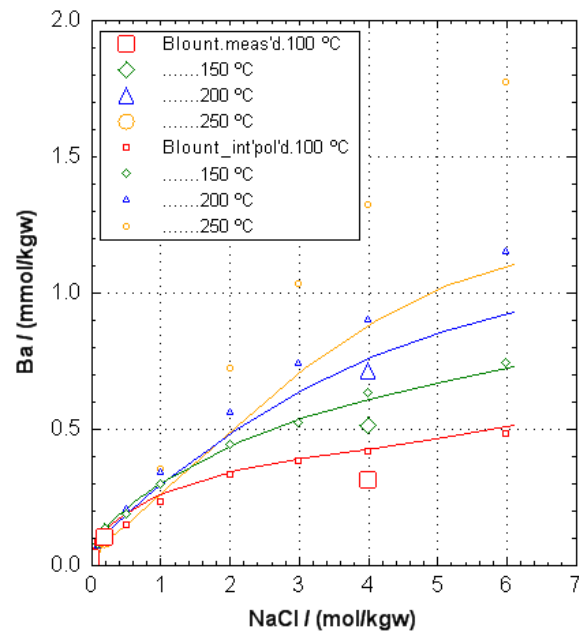


Figure A25. Solubility of barite ( $\text{BaSO}_4$ ) in NaCl solutions at 500 bar. Measured (large symbols) and interpolated (small symbols) data from Blount, 1977. File Barite\_500.phr.

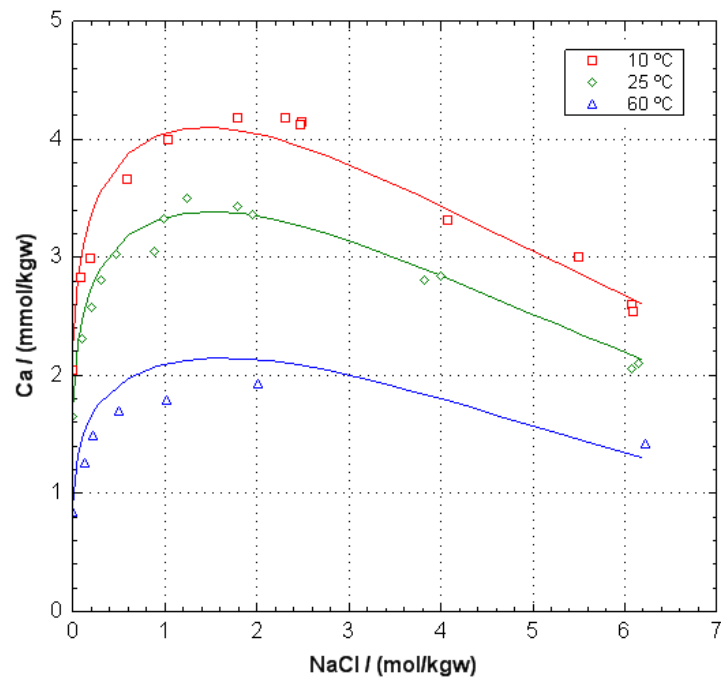


Figure A26. Solubility of calcite ( $\text{CaCO}_3$ ) in NaCl solutions at about 0.01 atm  $\text{CO}_2$  pressure. Measured data from Wolf et al., 1989. File cc\_Wolf.phr.

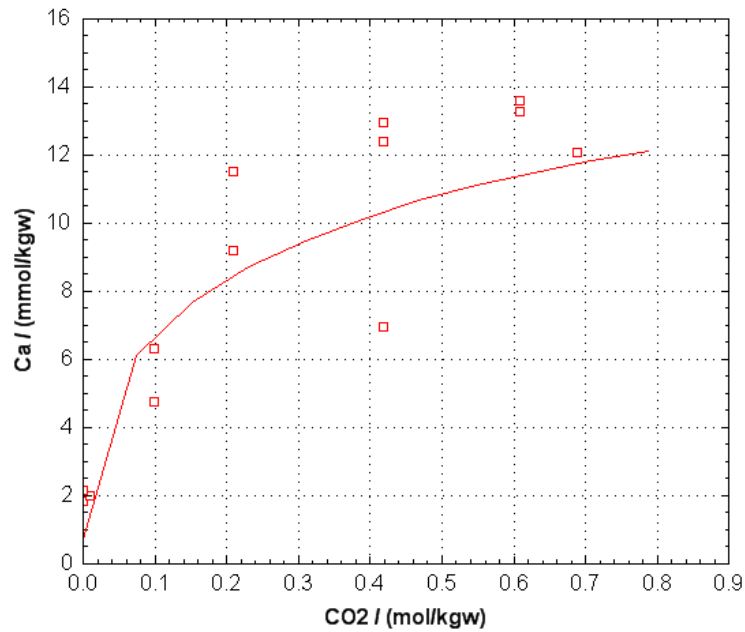


Figure A27. Solubility of calcite ( $\text{CaCO}_3$ ) at 200 °C, 580 atm pressure in 3 M NaCl as a function of the  $\text{CO}_2$  concentration. Measured data from Malinin and Kanukov, 1971. File cc\_Malin.phr.

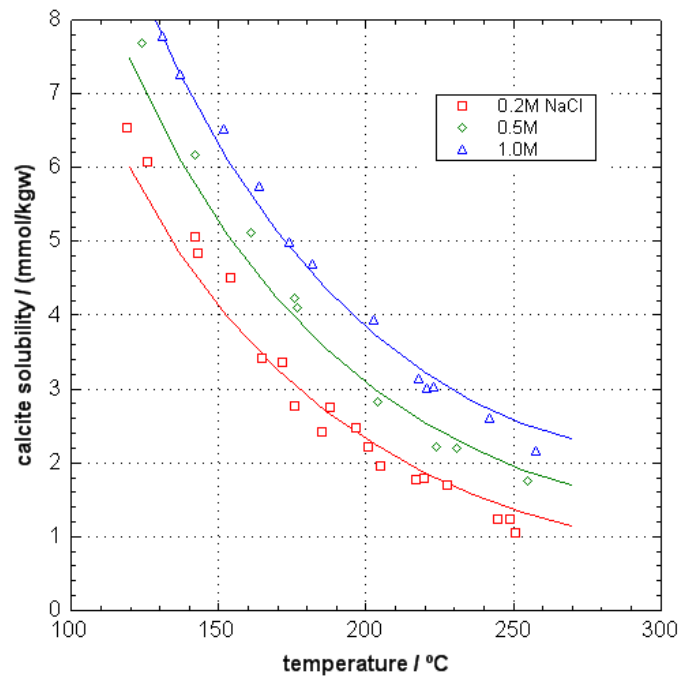


Figure A28. Solubility of calcite ( $\text{CaCO}_3$ ) in NaCl solutions at 12 bar  $\text{CO}_2$  pressure. Measured data from Ellis, 1963. File cc\_Ellis.phr.



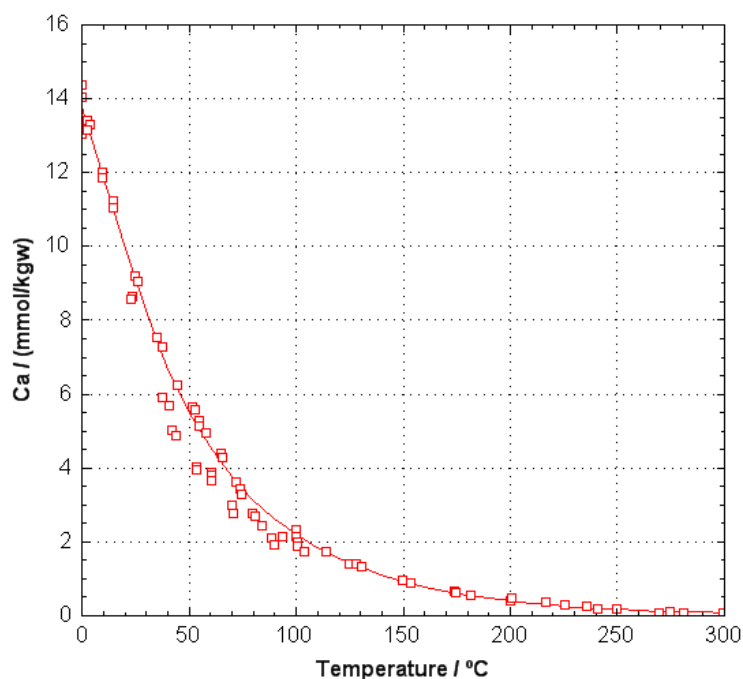


Figure A29. Solubility of calcite ( $\text{CaCO}_3$ ) as a function of temperature at 1 bar  $\text{CO}_2$  pressure. Measured data from Miller, 1952; Ellis, 1959; Plummer and Busenberg, 1982. File cc\_1barCO2.phr.

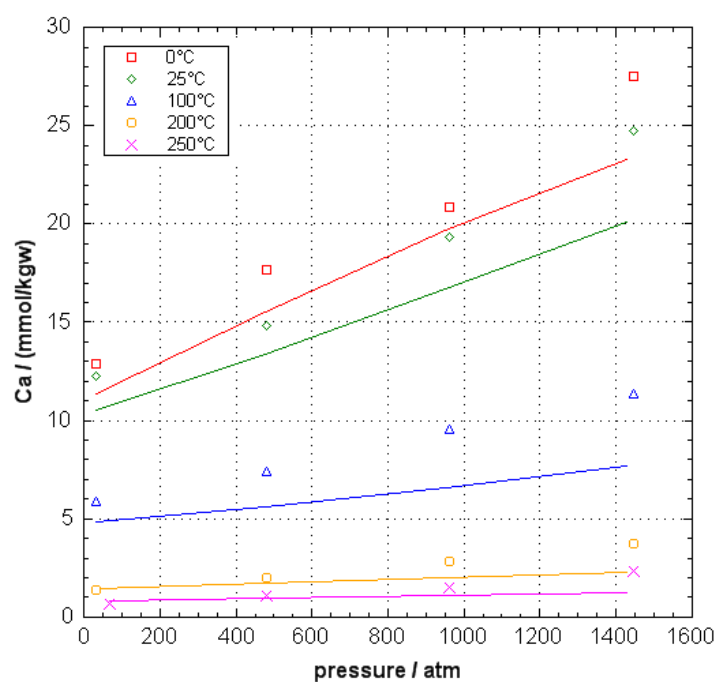


Figure A30. Solubility of calcite ( $\text{CaCO}_3$ ) in 0.1 M NaCl as a function of temperature and pressure at 1 bar  $\text{CO}_2$  pressure. Measured data from Shi et al., 2013. File cc\_Shi.phr. Solubilities at 4 M NaCl and in a brine are also calculated when the file is run.

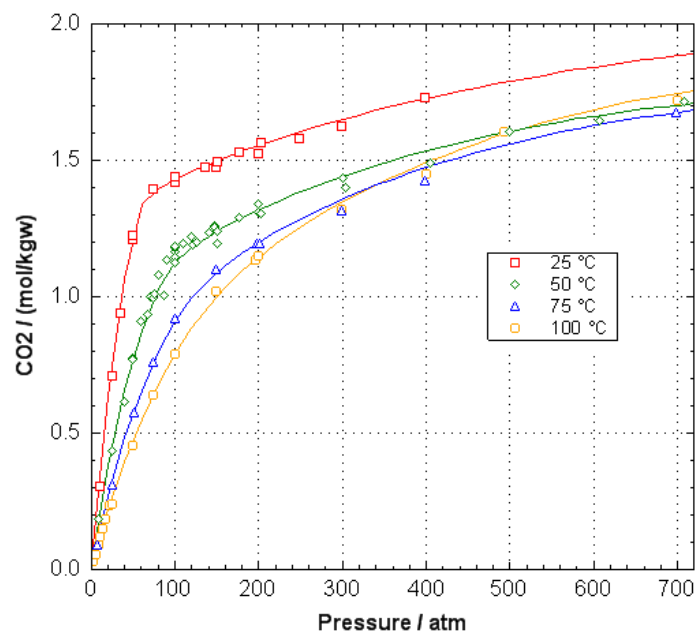


Figure A31. Solubility of CO<sub>2</sub> gas in water. Measured data from Wiebe and Gaddy, 1939, 1940; King et al., 1992; Takenouchi and Kennedy, 1964. File CO2\_conc\_PR\_IS.phr.

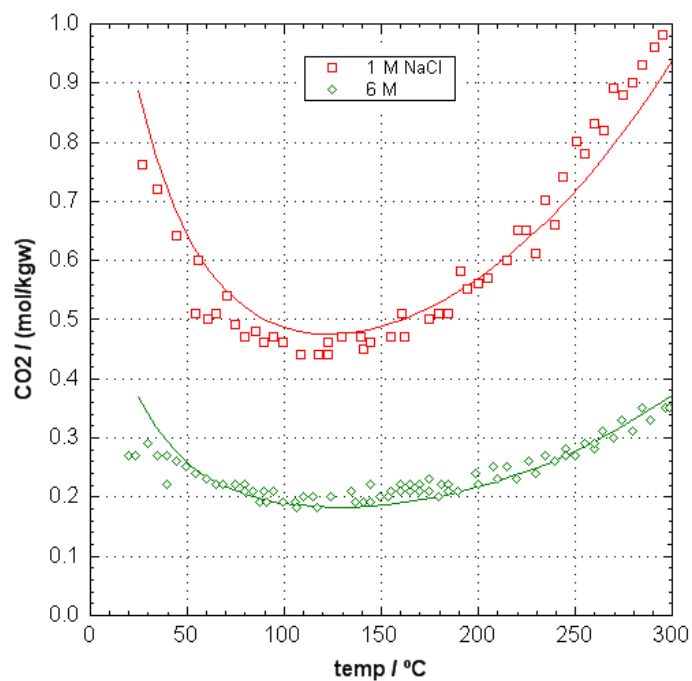


Figure A32. Solubility of CO<sub>2</sub> gas in 1 and 6 M NaCl solutions at about 40 atm CO<sub>2</sub>. Measured data from Drummond, 1981. File Drummond.phr.

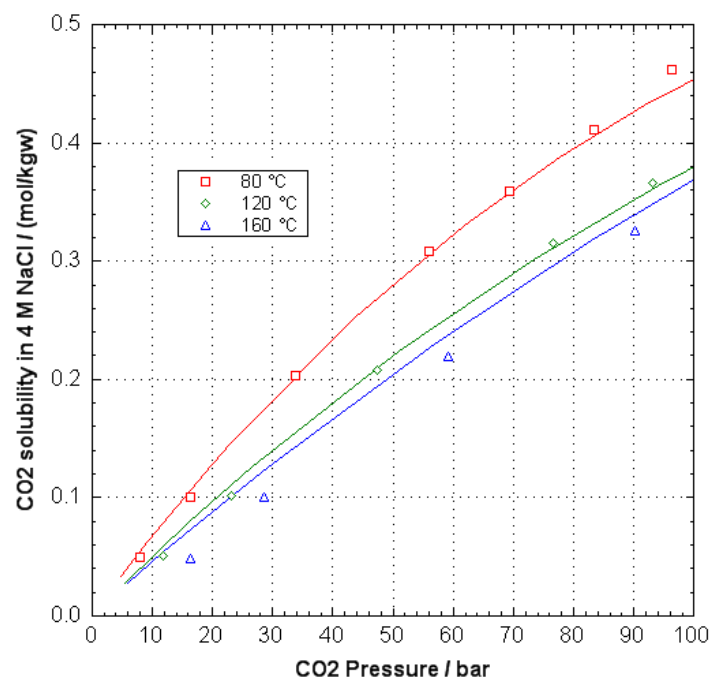


Figure A33. Solubility of CO<sub>2</sub> gas in 4 M NaCl solution. Measured data from Rumpf et al. 1994. File CO2\_4M\_NaCl.phr.

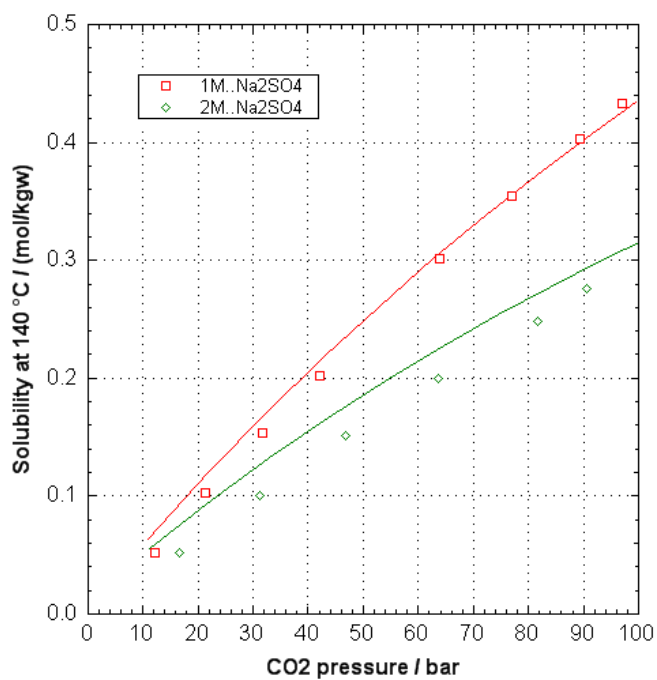


Figure A34. Solubility of CO<sub>2</sub> gas in Na<sub>2</sub>SO<sub>4</sub> solutions at 140°C. Measured data from Rumpf and Maurer, 1993. File P\_CO2\_Na2SO4.phr.

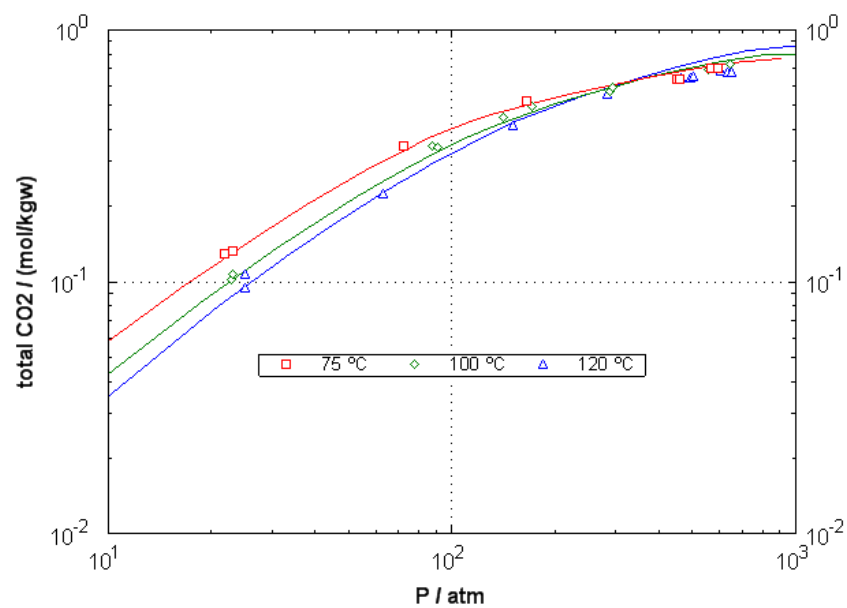


Figure A35. Solubility of CO<sub>2</sub> gas in 2.3 M CaCl<sub>2</sub> solution. Data from Springer et al., 2012. File CO2\_CaCl2.phr.

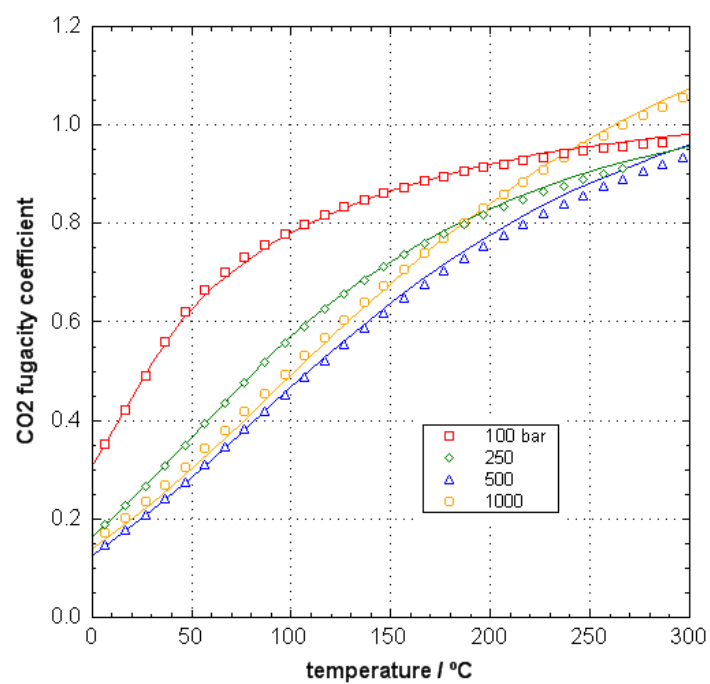


Figure A36. CO<sub>2</sub> fugacity coefficient as a function of temperature for CO<sub>2</sub> gas pressures from 100 - 1000 bar. Data from Angus et al., 1976. File phi\_Angus\_bar.phr.